MSUHEP-01213
CTEQ-016
hep-ph/0012261

Phenomenology of multiple parton radiation in semi-inclusive deep-inelastic scattering

P.M. Nadolsky[†], D. R. Stump[‡] and C.-P. Yuan [§]
Department of Physics and Astronomy, Michigan State University,
East Lansing, MI 48824, USA
(February 1, 2008)

Abstract

In the current region of semi-inclusive deep-inelastic scattering $l + A \to l' + B + X$, most events are accompanied by intensive radiation of soft and collinear partons which cannot be reliably described at any fixed order of perturbative QCD. In this paper, a resummation formalism that describes such multiple parton radiation is compared to the HERA data on semi-inclusive DIS, including the distributions of energy flow and charged particle multiplicity. We show that the resummation of multiple parton radiation improves the agreement between the theory and the data. We make some suggestions on further experimental study of multiple parton radiation at HERA.

[†]E-mail address: nadolsky@pa.msu.edu

[‡]E-mail address: stump@pa.msu.edu

[§]E-mail address: yuan@pa.msu.edu

I. INTRODUCTION

In a previous paper [1], we presented a formalism that enhances the predictive power of perturbative Quantum Chromodynamics (pQCD) with respect to the description of semi-inclusive hadroproduction at lepton-hadron colliders. We continue that study here, in part because new data has become available from HERA. The reaction that we consider is $l + A \to l' + B + X$, where l, A and l', B are initial- and final-state leptons and hadrons, respectively. Calculations in low orders of pQCD are only partially successful in explaining the abundant experimental data on semi-inclusive deep-inelastic scattering (sDIS) produced in recent years at the DESY-HERA ep collider [2–6]. Satisfactory agreement between the theory predictions and the experimental data requires scrupulous and systematic calculation of higher-order radiative corrections and, when necessary, all-order summation of poorly converging perturbative series. A formalism that was originally proposed in [8] and extended in [1] serves the latter purpose. It provides an improved theoretical description of nearly massless final-state hadrons that escape near the direction of the momentum of the electroweak vector boson exchanged between the leptonic and hadronic parts of the sDIS process. In other words, this formalism describes production of hadrons in the region of current fragmentation. In this kinematical regime, multiple radiation of soft and collinear partons is a dominant factor influencing the behavior of experimental observables. We have shown that the effects of multiple parton radiation are most evident in pseudorapidity spectra in the center-of-mass frame of the initial hadron and the exchanged electroweak boson.

The main goal of this paper is to demonstrate that resummation of large logarithmic corrections in the current region of sDIS improves the theoretical description of many aspects of this process. We compare predictions made within the resummation formalism to various sets of experimental data and to predictions obtained for these observables from a next-to-leading order (NLO) perturbative QCD calculation.

In Section II, we present the equations for the $\mathcal{O}(\alpha_s)$ and resummed cross sections that will be compared to experimental data in the subsequent Sections. In Section III, we compare theoretical predictions to new HERA data [4] on the energy flow in the hadronic center-of-mass reference frame. In Section IV, we discuss the impact of multiple parton radiation on various aspects of semi-inclusive charged particle production: in particular, resummation effects on transverse momentum distributions and on the correlation between the transverse and longitudinal momentum components of the observed final-state hadron. Section V contains our conclusions.

II. SUMMARY OF THE FIXED-ORDER AND RESUMMATION CALCULATIONS

In this paper we use notations and variables that were originally defined in Sections II and III of [1]. For the convenience of the reader, we briefly list the relevant definitions in Appendix A.

Following [7,8], we introduce a momentum scale q_T related to the space-like vector q_t^μ

given by

$$q_t^\mu = q^\mu - p_A^\mu \frac{q\cdot p_B}{p_A\cdot p_B} - p_B^\mu \frac{q\cdot p_A}{p_A\cdot p_B}. \tag{1}$$

The square of the scale q_T is defined by

$$q_T^2 = -q_t^\mu q_{t\mu}. \tag{2}$$

Throughout this paper we will consider observables in the hadronic center-of-mass (hCM) frame, in which the four-vector q_t^μ has a simple interpretation. This frame is defined by the condition $\vec{p}_A + \vec{q} = 0$. Let the direction of the z-axis in the hCM frame coincide with the direction of $\vec{q}$. Then the energy component and z component of q_t^μ vanish. The transverse components form a two-dimensional vector $\vec{q}_T$ that is simply the transverse momentum $\vec{p}_T$ of the final hadron B rescaled by the Lorentz scalar $-z \equiv -(p_B\cdot p_A)/(q\cdot p_A)$; that is,

$$q_t^\mu = \{0, \vec{q}_T, 0\} = \{0, -\frac{\vec{p}_T}{z}, 0\}. \tag{3}$$

The variable z controls the fragmentation of partons in the final state. Thus the vector $\vec{q}_T$ is closely related to the transverse momentum $\vec{p}_T$, except that it is not sensitive to the magnitude of the momentum vector $\vec{p}_B$, *i.e.,* not sensitive to the collinear final-state fragmentation. Rather, $\vec{q}_T$ determines the *direction* in which the final-state hadron is produced. In both the hadron Breit frame and the hCM frame, the magnitude of this vector q_T is a function of the pseudorapidity of the final-state hadron. In particular, we will later refer to the relationship between q_T and the pseudorapidity η^{cm} of the observed hadronic final state in the hCM frame, which is

$$q_T = We^{-\eta^{cm}}, \tag{4}$$

where $W^2 = (p_A+q)^2 = Q^2(1/x-1)$ is the square of the center-of-mass energy of the virtual photon and the proton. The multiple parton radiation that we are discussing here is important in the limit $\eta^{cm}\to+\infty$, or, equivalently, $q_T\to 0$.

To see how convergence of the perturbative series breaks down in the small-q_T region, we start by examining the hadron-level sDIS cross section $d\sigma_{BA}/(dxdzdQ^2dq_T^2d\varphi)$. This cross section can be expressed in terms of convolutions of parton-level cross sections $d\widehat{\sigma}_{ba}/(d\hat{x}d\hat{z}dQ^2dq_T^2d\varphi)$, and phenomenological long-distance hadronic functions:

$$\frac{d\sigma_{BA}}{dxdzdQ^2dq_T^2d\varphi} = \sum_{a,b}\int_z^1 \frac{d\xi_b}{\xi_b} D_{B/b}(\xi_b,\mu_F)\int_x^1 \frac{d\xi_a}{\xi_a} F_{a/A}(\xi_a,\mu_F)\frac{d\widehat{\sigma}_{ba}(\mu_F)}{d\hat{x}d\hat{z}dQ^2dq_T^2d\varphi}. \tag{5}$$

Here $F_{a/A}(\xi_a,\mu_F)$ denotes the parton distribution function (PDF) for a parton a in the hadron A, and $D_{B/b}(\xi_b,\mu_F)$ is the fragmentation function (FF) for the hadron B that is produced in the fragmentation of a parton b. The notation μ_F is used for the scale of factorization. The sum over the labels a,b includes contributions from all parton types, *i.e.,* $g,u,\bar{u},d,\bar{d},\ldots$. In the following, a sum over the indices i,j will include contributions from active flavors of quarks and antiquarks only, *i.e.,* it will not include a gluonic contribution.

Both the hadron-level and parton-level cross sections can be expanded into sums over leptonic angular functions $A_\rho(\psi,\varphi)$ (which are listed in Appendix A), as

$$\frac{d\sigma_{BA}}{dxdzdQ^2dq_T^2d\varphi} = \sum_{\rho=1}^{4} {}^{\rho}V_{BA}(x,z,Q^2,q_T^2)A_\rho(\psi,\varphi), \tag{6}$$

$$\frac{d\widehat{\sigma}_{ba}}{d\widehat{x}d\widehat{z}dQ^2dq_T^2d\varphi} = \sum_{\rho=1}^{4} {}^{\rho}\widehat{V}_{ba}(\widehat{x},\widehat{z},Q^2,q_T^2)A_\rho(\psi,\varphi). \tag{7}$$

The coefficients ${}^{\rho}V_{BA}$ (or ${}^{\rho}\widehat{V}_{ba}$) of the angular functions $A_\rho(\psi,\varphi)$ are independent of one another. If $q_T/Q \ll 1$, but $q_T \neq 0$, the perturbative parton-level cross section is dominated by the term with $\rho = 1$. The structure function for this term ${}^{1}\widehat{V}_{ba}(\widehat{x},\widehat{z},Q^2,q_T^2)$ behaves as $1/q_T^2$ times a series in powers of α_s and logarithms $\ln(q_T^2/Q^2)$,

$${}^{1}\widehat{V}_{ba}(\widehat{x},\widehat{z},Q^2,q_T^2) \approx \frac{\sigma_0 F_l}{2\pi S_{eA}}\frac{1}{q_T^2}\sum_{k=1}^{\infty}\left(\frac{\alpha_s}{\pi}\right)^k \sum_{m=0}^{2k-1}\widehat{v}_{ba}^{(km)}(\widehat{x},\widehat{z})\ln^m\left(\frac{q_T^2}{Q^2}\right). \tag{8}$$

The constants σ_0 and F_l, which were introduced in [1], are

$$\sigma_0 \equiv \frac{Q^2}{4\pi S_{eA}x^2}\left(\frac{e^2}{2}\right), \tag{9}$$

$$F_l = \frac{e^2}{2}\frac{1}{Q^2}. \tag{10}$$

The coefficients $\widehat{v}_{ba}^{(km)}(\widehat{x},\widehat{z})$ are generalized functions of the variables $\widehat{x}$ and $\widehat{z}$.

Convergence of the series in (8) deteriorates rapidly as $q_T/Q \to 0$, because of the growth of the terms $(q_T^{-2})\ln^m(q_T^2/Q^2)$. As a result, the structure function ${}^{1}\widehat{V}_{ba}(\widehat{x},\widehat{z},Q^2,q_T^2)$ has a non-integrable singularity at $q_T = 0$. Its asymptotic behavior is very different from that of the structure functions ${}^{2,3,4}\widehat{V}_{ba}(\widehat{x},\widehat{z},Q^2,q_T^2)$, which are less singular and, in fact, integrable at $q_T = 0$. This singular behavior of ${}^{1}\widehat{V}_{ba}(\widehat{x},\widehat{z},Q^2,q_T^2)$ is generated by infrared singularities of the perturbative cross section that are located at $q_T = 0$. These singularities must be either explicitly canceled or factored into the long-distance hadronic functions in order to obtain a finite cross section.

There exist two qualitatively different approaches for handling such singularities. The first approach deals with the singularities order by order in perturbation theory; the second approach identifies and sums the most singular terms in all orders of the perturbative expansion. We will begin by discussing the first approach, in which singularities are regularized independently at each order of the series in α_s. In the crudest approximation, one keeps only terms of the order $\mathcal{O}(\alpha_s)$ and drops all higher-order terms. The singularity in the $\mathcal{O}(\alpha_s)$ part of the asymptotic expansion (8) can be regularized by introducing a "separation scale" q_T^{sep} and considering the fixed-order cross section separately in the regions $0 \le q_T \le q_T^{sep}$ and $q_T > q_T^{sep}$. The value of q_T^{sep} should be small enough for the approximation (8) to be valid over the whole range $q_T \le q_T^{sep}$.

In the region $0 \le q_T \le q_T^{sep}$, we can apply the $\overline{MS}$ factorization scheme to take care of the singularities at $q_T = 0$. In the $\overline{MS}$ scheme, the regularization is done through continuation

of the parton-level cross section to $n = 4 - 2\varepsilon$ dimensions. The n-dimensional expression for the asymptotic expansion (8) of ${}^1\widehat{V}_{ba}(\widehat{x}, \widehat{z}, Q^2, q_T^2)$ is

$$ {}^1\widehat{V}_{ba}(\widehat{x}, \widehat{z}, Q^2, q_T^2) \approx \frac{\sigma_0 F_l}{2\pi S_{eA}} \left(\frac{2\pi\mu}{\widehat{z}}\right)^{4-n} \frac{1}{q_T^2} \sum_{k=1}^{\infty} \left(\frac{\alpha_s}{\pi}\right)^k \sum_{m=0}^{2k-1} \widehat{v}_{ba}^{(km)}(\widehat{x}, \widehat{z}) \ln^m\left(\frac{q_T^2}{Q^2}\right). \tag{11} $$

The scale parameter μ in (11) is introduced to restore the correct dimensionality of the parton-level cross section $d\widehat{\sigma}_{ba}/(d\widehat{x}d\widehat{z}dQ^2 dq_T^{n-2} d\varphi)$. The soft and collinear singularities appear as terms proportional to $1/\varepsilon^n$ when $n \to 4$. The soft singularity in the real emission corrections cancels with the soft singularity in the virtual corrections. The remaining collinear singularities are absorbed into the partonic PDFs and FFs, which therefore must be redefined at each order of the perturbative calculation. When the partonic PDFs and FFs are subtracted from the partonic cross section $d\widehat{\sigma}$, the remainder is finite and independent of the types of the external hadrons. We denote this finite remainder as $(d\widehat{\sigma})_{hard}$. The convolution of $(d\widehat{\sigma})_{hard}$ with the hadronic PDFs and FFs yields a cross section for the external hadronic states A and B. There is a certain freedom in the precise definition of the collinear contributions, so that the "hard" part depends on an arbitrary factorization scale μ_F through terms like $P_{ab} \ln(\mu_F/K)$, where $P_{ab}(\xi)$ are $\mathcal{O}(\alpha_s)$ splitting functions [9], and K is some momentum scale in the process.[1] The dependence on the factorization scale in the hard part is compensated, up to higher-order terms in α_s, by scale dependence of the long-distance hadronic functions.[2]

After the cancellation of soft singularities and factorization of collinear singularities, one can calculate analytically the integral of $({}^1\widehat{V}_{ba})_{hard}$ over the region $0 \le q_T \le q_T^{sep}$. At $\mathcal{O}(\alpha_s)$ this integral is given by

$$ \int_0^{(q_T^{sep})^2} dq_T^2 \left({}^1\widehat{V}_{ba}\right)_{hard} = \frac{\sigma_0 F_l}{S_{eA}} \sum_j e_j^2 \left\{ {}^1\widehat{V}_{ba,j}^{LO} + \frac{\alpha_s(\mu'_F)}{\pi} {}^1\widehat{V}_{ba,j}^{NLO} \right\}, \tag{12} $$

where $j = u, \bar{u}, d, \bar{d}, \ldots$; the LO and NLO structure functions are

$$ {}^1\widehat{V}_{ba,j}^{LO} = \delta(1-\widehat{z})\delta(1-\widehat{x})\delta_{bj}\delta_{ja}, \tag{13} $$

$$ \begin{aligned} {}^1\widehat{V}_{ba,j}^{NLO} &= -\frac{1}{2}\left[\left(C_F \ln^2 \frac{Q^2}{(q_T^{sep})^2} - 3C_F \ln \frac{Q^2}{(q_T^{sep})^2}\right)\delta(1-\widehat{z})\delta(1-\widehat{x})\delta_{bj}\delta_{ja}\right. \\ &\quad + \left. \ln \frac{\mu_F^2}{(\widehat{z}\, q_T^{sep})^2}\Big(\delta(1-\widehat{z})\delta_{bj}P_{ja}(\widehat{x}) + P_{bj}(\widehat{z})\delta(1-\widehat{x})\delta_{ja}\Big)\right] \\ &\quad + \delta(1-\widehat{z})\delta_{bj} c_{ja}^{in(1)}(\widehat{x}) + c_{bj}^{out(1)}(\widehat{z})\delta(1-\widehat{x})\delta_{ja}. \end{aligned} \tag{14} $$

---

[1] The scales μ_F and μ are related as $\mu_F^2 = 4\pi e^{-\gamma_E}\mu^2$, where γ_E is the Euler constant.

[2] In our calculations we do not distinguish between factorization scales for PDFs and FFs nor between the factorization and renormalization scales.

The coefficient functions $c_{ba}^{in,out(1)}(\xi)$ that appear in ${}^1\widehat{V}_{ba,j}^{NLO}$ are given by

$$c_{ji}^{(1)in}(\xi) = c_{ij}^{out(1)}(\xi) \;=\; \delta_{ij}C_F\left[\frac{1}{2}(1-\xi) - 2\delta(1-\xi)\right], \tag{15}$$

$$c_{jg}^{(1)in}(\xi) \;=\; \frac{1}{2}\xi(1-\xi), \tag{16}$$

$$c_{gj}^{(1)out}(\xi) \;=\; \frac{C_F}{2}\xi. \tag{17}$$

Now consider the kinematical region $q_T > q_T^{sep}$, where the approximation (11) no longer holds. In this region, $({}^1\widehat{V}_{ba})_{hard}$ should be obtained from the exact NLO result. With this prescription, the integral over q_T^2 can be calculated as

$$\begin{aligned}\int_0^{\max q_T^2} dq_T^2 \frac{d\widehat{\sigma}_{ba}}{d\widehat{x}d\widehat{z}dQ^2dq_T^2d\varphi} \;&=\; \\ A_1(\psi,\varphi)\left\{\int_0^{(q_T^{sep})^2} dq_T^2 \left({}^1\widehat{V}_{ba}\right)_{hard} \;+\; \int_{(q_T^{sep})^2}^{\max q_T^2} dq_T^2 \left({}^1\widehat{V}_{ba}\right)_{hard}\right\} \\ &+\; \sum_{\rho=2}^{4} A_\rho(\psi,\varphi) \int_0^{\max q_T^2} dq_T^2 \left({}^\rho\widehat{V}_{ba}\right),\end{aligned} \tag{18}$$

where $\max q_T^2$ is the maximal value of q_T^2 allowed by kinematics. The first integral on the right-hand side is calculated analytically, using the approximation (12); the second and third integrals are calculated numerically, using the complete perturbative result of the order $\mathcal{O}(\alpha_s)$. The numerical calculation is done with the help of a Monte Carlo integration program written in the style of the package ResBos used earlier for resummation in vector boson production at hadron-hadron colliders [10].

A significant failure of the calculational procedure in (18) is that it does not reproduce the correct shape of q_T-dependent differential cross sections in the region $q_T \ll Q$. The fundamental problem is that the terms in (11) with small powers of α_s do not reliably approximate the complete sum in the region $q_T \ll Q$, where the large magnitudes of the logarithmic terms $\ln^m(q_T^2/Q^2)$ quickly invalidate the expansion in powers of α_s. In other words, a truncated sum in powers of α_s (*cf.* Eq. (12)) cannot be a reliable prediction for the observable cross section in the region $q_T/Q \ll 1$.

The problem mentioned in the previous paragraph justifies the second approach to the regularization of the singularities at $q_T = 0$, in which large logarithms in (11) are summed to all orders. According to the formalism developed in [11,12] and adapted to the sDIS process in [8], a better approximation for this sum is provided by the Fourier transform of a $\vec{b}$-space function $\widetilde{W}(b,Q,\widehat{x},\widehat{z},C_1,C_2,\mu_F)$, which sums the dominant terms in (8) through all orders of α_s:

$${}^1\widehat{V}_{ba}(\widehat{x},\widehat{z},Q^2,q_T^2) = \frac{\sigma_0 F_l}{2S_{eA}} \int \frac{d^2b}{(2\pi)^2} e^{i\vec{q}_T\cdot\vec{b}} \widetilde{W}_{ba}(b,Q,\widehat{x},\widehat{z},C_1,C_2,\mu_F). \tag{19}$$

Here $\vec{b}$ is a vector conjugate to $\vec{q}_T$, and b denotes the magnitude of $\vec{b}$.

From first principles [11,12], the general structure of $\widetilde{W}_{ba}(b,Q,\widehat{x},\widehat{z},C_1,C_2,\mu_F)$ is known to have the form

$$\widetilde{W}_{ba}(b,Q,\widehat{x},\widehat{z},C_1,C_2,\mu_F) =$$

$$\sum_j e_j^2 \mathcal{C}_{bj}^{out}(\widehat{z},C_1,C_2,b_*,\mu_F) e^{-S^P(b_*,Q,C_1,C_2)} e^{-S^{NP}} \mathcal{C}_{ja}^{in}(\widehat{x},C_1,C_2,b_*,\mu_F), \tag{20}$$

where $j = u,\bar{u},d,\bar{d},\ldots$. The meanings of various factors in Eq. (20) were discussed in detail in [1]. Here we should emphasize that at short distances, *i.e.*, in the limit $b \to 0$, the function $\widetilde{W}_{ba}(b,Q,\widehat{x},\widehat{z},C_1,C_2,\mu_F)$ is dominated by perturbatively calculable functions $\mathcal{C}_{ja}^{in}(\widehat{x},C_1,C_2,b,\mu_F)$, $\mathcal{C}_{bj}^{out}(\widehat{z},C_1,C_2,b,\mu_F)$, and the perturbative part of the Sudakov factor $S^P(b,Q,C_1,C_2)$. The $\mathcal{O}(\alpha_s)$ expressions for these functions are listed in Appendix B.

In the region $b \gtrsim b_{max}$, where b_{max} can be chosen to be $0.5\ \mathrm{GeV}^{-1}$, nonperturbative contributions to $\widetilde{W}_{ba}$ become important. These nonperturbative contributions are absorbed into a function $S^{NP}(b,Q,\ldots)$, which vanishes in the limit $b \to 0$ but dominates $\widetilde{W}_{ba}(b,Q,\widehat{x},\widehat{z},C_1,C_2,\mu_F)$ for $b \gtrsim b_{max}$. Until a nonperturbative theory of strong interactions is developed, the explicit parametrization of $S^{NP}(b,Q,\ldots)$ can only be found from comparison with experimental data. One possible realization of a smooth transition in the region $b \sim b_{max}$ between the perturbative and nonperturbative parts of $\widetilde{W}_{ba}(b,Q,\widehat{x},\widehat{z},C_1,C_2,\mu_F)$ is to replace the parameter b in the $\mathcal{C}$-functions and the perturbative Sudakov factor S^P by the variable

$$b_* \equiv \frac{b}{\sqrt{1+(b/b_{max})^2}}, \tag{21}$$

as written in (20).

There is a subtle difference between $\mathcal{C}^{in}$ and $\mathcal{C}^{out}$. While the initial-state coefficient functions $\mathcal{C}_{ba}^{in(1)}(\widehat{x},C_1,C_2,b,\mu_F)$ given in Eqs. (70) and (71) depend on the factorization scale μ_F through a factor $\ln[\mu_F b/b_0]$, the final-state functions $\mathcal{C}_{ba}^{out(1)}(\widehat{z},C_1,C_2,b,\mu_F)$ given in Eqs. (72) and (73) depend instead on $\ln[\mu_F b/(b_0\widehat{z})]$. The additional term $\propto \ln\widehat{z}$ in the functions $\mathcal{C}_{ba}^{out(1)}(\widehat{z},C_1,C_2,b,\mu_F)$ becomes large and negative when $\widehat{z} \to 0$, so that it can significantly influence the $\mathcal{O}(\alpha_s)$ contribution at small values of $\widehat{z}$. As a result, the resummed total rate tends to be lower than its fixed-order counterpart for $z \lesssim 0.1$. We will discuss this issue in more detail in Section IV. Similarly, the $\mathcal{O}(\alpha_s)$ part of the NLO structure function ${}^1\widehat{V}_{ba,j}^{NLO}$ in (14) depends on μ_F through a logarithm $\ln[\mu_F^2/(\widehat{z}q_T^{sep})^2]$.

The appearance of the additional terms $\propto \ln\widehat{z}$ in the functions $\mathcal{C}_{bj}^{out(1)}$ and ${}^1\widehat{V}_{ba,j}^{NLO}$ reflects the specifics of separation of the $\mathcal{O}(\alpha_s)$ "hard" cross section $(\widehat{\sigma})_{hard}$ from the collinear contributions to the FFs in the $\overline{MS}$ factorization scheme. The easiest way to see the specific origin of the $\ln\widehat{z}$ terms is to notice that the dependence on the parameter μ in the n-dimensional expression (11) for ${}^1\widehat{V}_{ba}(\widehat{x},\widehat{z},Q^2,q_T^2)$ comes through a factor $(2\pi\mu/\widehat{z})^{4-n}$, rather than through a more conventional $(2\pi\mu)^{4-n}$. It is this factor that generates the μ_F-dependent logarithmic terms $\ln[\mu_F b/(b_0\widehat{z})]$ in the functions $\mathcal{C}_{bj}^{out(1)}(\widehat{z},C_1,C_2,b,\mu_F)$ and ${}^1\widehat{V}_{ba,j}^{NLO}$. The $\mathcal{C}_{ja}^{in(1)}$-functions do not include $\ln\widehat{z}$ because they are evaluated along the direction $\widehat{z}=1$ in the phase space. In

contrast, nothing forbids such a term in the functions $\mathcal{C}_{bj}^{out(1)}$, in which $\widehat{z}$ can be anything between z and 1. This contribution produces terms of the form $P_{bj} \ln \widehat{z}$ in $\mathcal{C}_{bj}^{out(1)}(\widehat{z}, C_1, C_2, b, \mu_F)$, which suppress the resummed rate for the production of hadrons with very small energies.

In Ref. [1], the terms proportional to $\ln \widehat{z}$ were left out of the expressions for the $\mathcal{C}_{ba}^{out}$-functions. This error affected the value of the $\mathcal{C}^{out}$-function for the energy flow in Ref. [1]; the correct expression is Eq. (30) in this paper. We have found that theoretical distributions that were shown in the Figures of Ref. [1] will be approximately reproduced with the correct $\mathcal{C}_{ba}^{out}$ if the following nonperturbative Sudakov factor is used:

$$S_z^{NP}(b) = g_{BA}^{(2)}(b) \ln \frac{Q}{Q_0} + b^2 \Big(-4.58 + \frac{0.58}{\sqrt{x}} \Big). \tag{22}$$

The explicit parametrization for the coefficient $g_{BA}^{(2)}(b)$ is given in [1]. In the next Section, we present an updated analysis of the transverse energy flow that is compared to the newer data from the H1 Collaboration. We will present a new parametrization of the nonperturbative Sudakov factor which is in better agreement with the whole set of experimental data.

III. RESUMMATION FOR THE TRANSVERSE ENERGY FLOW

As was discussed at length in [1], knowledge of the resummed semi-inclusive DIS cross section leads immediately to predictions for the pseudorapidity spectrum of the transverse energy flow in the hadron Breit frame or the hCM frame. It is advantageous to study the energy flows, because they are less dependent on the specifics of final-state fragmentation of the scattered partons into the observed hadrons. We therefore start the presentation of our numerical results with the comparison of the resummation formalism to the experimentally measured pseudorapidity distributions for the transverse energy flow in the hCM frame.

According to Eq. (4), the scale q_T for massless particles is simply related to the pseudorapidity η^{cm} in the hCM frame, if the energy of the photon-proton collision is fixed. Therefore the pseudorapidity distribution for the transverse energy flow in the hCM frame $d\langle E_T \rangle / d\eta^{cm}$ can be converted into a q_T-distribution $d\langle E_T \rangle / dq_T$ by a simple change of variables. From the viewpoint of theoretical analysis, it is preferable to convert $d\langle E_T \rangle / d\eta^{cm}$ into the q_T distribution of the "z-flow" [13] that is defined as

$$\frac{d\Sigma_z}{dx\, dQ^2\, dq_T} = \sum_B \int_{z_{min}}^1 z \, \frac{d\sigma(e + A \to e + B + X)}{dx\, dz\, dQ^2\, dq_T} \, dz. \tag{23}$$

Under the approximation that all particles are massless, the distribution $d\langle E_T \rangle / d\eta^{cm}$ is simply related to the distribution $d\Sigma_z / dq_T$, by

$$\frac{d\langle E_T \rangle}{d\eta_{cm}} = q_T^2 \frac{d\Sigma_z}{dq_T}. \tag{24}$$

In [1] the predictions of the resummation formalism were compared to data on transverse energy flow $\langle E_T \rangle$ published in [3]. In a recent publication [4], the H1 Collaboration at the DESY-HERA ep collider presented new data on the distributions $d\langle E_T \rangle / d\eta^{cm}$ in the same

bins of x and Q^2 as in [3] and, in addition, in several bins at significantly higher x and Q^2. In this paper, we repeat the analysis of [1] to produce distributions $d\Sigma_z/dq_T$ for the bins of x and Q^2 discussed in [4]. The procedure of our numerical analysis is identical to the one used in [1]. Our calculations use the parameters of the HERA ep collider. The energies of the proton and electron beams are taken to be 820 GeV and 27.5 GeV, respectively. The current numerical results are obtained using CTEQ5M1 parton distribution functions [16].

By the factorization theorems of QCD, the hadron-level z-flow Σ_z can be written as the convolution of a parton-level z-flow $\widehat{\Sigma}_z$ with the PDFs,

$$\frac{d\Sigma_z}{dxdQ^2dq_T^2d\varphi} = \sum_a \int_x^1 \frac{d\xi_a}{\xi_a} F_{a/A}(\xi_a,\mu_F) \frac{d\widehat{\Sigma}_z(\mu_F)}{d\widehat{x}dQ^2dq_T^2d\varphi}. \tag{25}$$

Similarly to the sDIS cross section, the z-flow can be expanded in a sum over the leptonic angular functions $A_\rho(\psi,\varphi)$:

$$\frac{d\widehat{\Sigma}_z}{d\widehat{x}dQ^2dq_T^2d\varphi} = \sum_{\rho=1}^{4} {}^{\rho}\widehat{V}_{za}(\widehat{x},Q^2,q_T^2) A_\rho(\psi,\varphi), \tag{26}$$

where the structure functions ${}^{\rho}\widehat{V}_{za}(\widehat{x},Q^2,q_T^2)$ for the z-flow are related to the structure functions ${}^{\rho}\widehat{V}_{ba}(\widehat{x},\widehat{z},Q^2,q_T^2)$ for the sDIS cross section by

$${}^{\rho}\widehat{V}_{za}(\widehat{x},Q^2,q_T^2) = \sum_b \int_0^1 \widehat{z}d\widehat{z}\ {}^{\rho}\widehat{V}_{ba}(\widehat{x},\widehat{z},Q^2,q_T^2). \tag{27}$$

The resummed z-flow is calculated as

$$\frac{d\Sigma_z}{dxdQ^2dq_T^2d\varphi} = \frac{\sigma_0 F_l}{S_{eA}} \frac{A_1(\psi,\varphi)}{2} \int \frac{d^2b}{(2\pi)^2} e^{i\vec{q}_T\cdot\vec{b}} \widetilde{W}_z(b,x,Q) + Y_z, \tag{28}$$

where

$$\widetilde{W}_z(b,x,Q) = \sum_j e_j^2 \mathcal{C}_z^{out}\, e^{-S_z(b,Q,x)}\, (\mathcal{C}_{ja}^{in} \circ F_{a/A})(x,b_*,\mu_F). \tag{29}$$

The functions $\mathcal{C}_{ja}^{in}$ in (29) are the same as in (20). The coefficient $\mathcal{C}_z^{out}$ is

$$\mathcal{C}_z^{out} = 1 + \frac{\alpha_s}{\pi} C_F \Big(-\frac{7}{16} - \frac{\pi^2}{3} - \ln^2 \frac{e^{-3/4} C_1}{C_2 b_0}\Big), \tag{30}$$

where $b_0 \equiv 2e^{-\gamma_E}$ and $\gamma_E = 0.577\ldots$ is the Euler constant. The parameter b_*, given by (21) with $b_{max} = 0.5\ \mathrm{GeV}^{-1}$, is introduced in (29) to smoothly turn off the perturbative dynamics when b exceeds b_{max}. The numerical results for the resummed z-flow are obtained using $C_1/C_2 = \mu_F b = b_0$.

The term Y_z in (28) is the difference between the complete fixed-order expression at $\mathcal{O}(\alpha_s)$ for $d\Sigma_z/(dxdQ^2dq_T^2d\varphi)$ and its most singular part in the limit $q_T \to 0$; that is,

$$Y_z = \frac{d\Sigma_z}{dxdQ^2dq_T^2d\varphi} - \left(\frac{d\Sigma_z}{dxdQ^2dq_T^2d\varphi}\right)_{sing}. \tag{31}$$

The singular part calculated to $\mathcal{O}(\alpha_s)$ is

$$\left(\frac{d\Sigma_z}{dxdQ^2dq_T^2d\varphi}\right)_{sing} = \frac{\sigma_0 F_l}{S_{eA}}\frac{\alpha_s}{\pi}\frac{1}{2q_T^2}\frac{A_1(\psi,\varphi)}{2\pi} \times \sum_j e_j^2\Bigg[\Big\{(P_{qq}\circ F_{j/A})(x,\mu_F)+(P_{qg}\circ F_{g/A})(x,\mu_F)\Big\} + 2F_{j/A}(x,\mu_F)\Big\{C_F\ln\frac{Q^2}{q_T^2}-\frac{3}{2}C_F\Big\}+\mathcal{O}\Big(\Big(\frac{\alpha_s}{\pi}\Big)^2,q_T^2\Big)\Bigg]. \quad (32)$$

The formula (28) is expected to provide a smooth matching between the resummed z-flow in the region $q_T \ll Q$ and the fixed-order z-flow in the region $q_T \gtrsim Q$. However, we find that the $\mathcal{O}(\alpha_s)$ fixed-order z-flow significantly undershoots the data in the region $q_T/Q \gtrsim 1$. The resummed z-flow shows better agreement with the data, over a wide range of q_T/Q, but also lies below the data if q_T/Q significantly exceeds unity. The discrepancy between the theoretical z-flows and the data at $q_T/Q \gtrsim 1$ is illustrated for the bin $\langle Q^2\rangle = 33.2$ GeV^2, $\langle x\rangle = 0.0047$ in Fig. 1 and for the bin $\langle Q^2\rangle = 617$ GeV^2, $\langle x\rangle = 0.026$ in Fig. 2. The data at sufficiently high q_T lies above the $\mathcal{O}(\alpha_s)$ z-flow and the resummed z-flow in both bins. This difference signals that calculation of higher order radiative corrections is required to achieve agreement between the theory and the data for $q_T/Q \gtrsim 1$. The better consistency between the resummed z-flow and the data suggests that we should use the resummed z-flow up to values of $q_T/Q \sim 1$, *i.e.,* without switching to the fixed-order expression. We have followed this procedure in the derivation of our numerical results.

We have also found that the agreement between the resummed z-flow and the data in the region $q_T/Q \sim 1$ can be improved by making an additional correction that accounts for the reduction of the allowed phase space with the increase of q_T. This correction was discussed in detail in [1]. Its importance can be understood by noting the steep rise of the PDFs as x decreases, at values of x relevant to the HERA measurements. This steep rise in the small x region, together with a mismatch between the phase space in the b-space integral of the resummed z-flow (28) and that in the exact fixed-order formula, may produce large numerical effects if q_T is of the order Q or larger. To correct for this mismatch between the resummation and the perturbative phase spaces, $x = Q^2/(2p_A\cdot q)$ is replaced in Eqs. (29) and (32) by the q_T-dependent quantity

$$\widetilde{x} = \frac{Q^2+q_T^2}{Q^2}x. \quad (33)$$

The replacement $x \to \widetilde{x}$ preserves the leading-order kinematics when q_T approaches zero; at the same time, it simulates the reduction of the allowed phase space when q_T becomes comparable with Q. It affects only the convolution integrals $(P_{ba}\circ F_{a/A})$ and $(\mathcal{C}_{ba}\circ F_{a/A})$, in which the q_T-independent lower limit of integration x is replaced by the variable $\widetilde{x}$. The result of this replacement is that the convolution integrals at large q_T do not include large contributions from very small values of x, which helps to improve the accuracy of the matching procedure at $q_T \sim Q$.

Before turning to the discussion of the experimental data, let us comment on the structure of the Sudakov factor $S_z(b,Q,x)$ in (29). As in the case of the sDIS cross section, the Sudakov

factor for the z-flow consists of both perturbative and nonperturbative parts,

$$S_z(b,Q,x) \;=\; \int_{C_1^2/b_*^2}^{C_2^2Q^2} \frac{d\overline{\mu}^2}{\overline{\mu}^2}\left(A(\alpha_s(\overline{\mu}),C_1)\ln\frac{C_2^2Q^2}{\overline{\mu}^2} + B(\alpha_s(\overline{\mu}),C_1,C_2)\right) \\ +\; S_z^{NP}(b,Q,x). \tag{34}$$

A realistic parametrization for the nonperturbative Sudakov factor $S_z^{NP}(b,Q,x)$ can be obtained by comparison with experimental data, especially with the measured pseudorapidity distributions at $Q \approx 3-20$ GeV. As Q increases, we expect the data to become less sensitive to nonperturbative effects and to be dominated by perturbatively calculable parton radiation. In [1] we found a parametrization of $S_z^{NP}(b,Q,x)$ that was consistent with the data published in [3]. But, because of the limited scope of those data, that parametrization was expected to be valid only for $10^{-4} \le x \le 10^{-2}$. Also, the Q dependence of $S_z^{NP}(b,Q,x)$ could not be tested, since all the pseudorapidity distributions in Ref. [3] were presented in a small range of $Q \approx 2-6$ GeV. Hence, the parametrization of $S_z^{NP}(b,Q,x)$ in [1] used a model prediction for the coefficient of $\ln Q/Q_0$ based on the assumption of crossing symmetry between the nonperturbative Sudakov factors in sDIS, e^+e^- hadroproduction, and Drell-Yan processes.

In its more recent publication [4], the H1 Collaboration presented pseudorapidity distributions of the transverse energy flow for Q^2 up to 2200 GeV^2. However, as just mentioned, the data at such high Q^2 should be rather insensitive to the nonperturbative dynamics, *e.g.,* because the nonperturbative effects would be important only at very large values of η^{cm}, for which the resolution of the detector is poor. Thus the data at very high Q^2 is not very informative about the Q^2-dependence of $S_z^{NP}(b,Q,x)$ either. To learn about the dependence on Q^2, one needs to look at data in the range $Q \sim 5-20$ GeV. Fortunately, the H1 Collaboration presented distributions in two bins at intermediate values of $\langle Q^2\rangle$, namely $\langle Q^2\rangle = 59.4$ GeV^2 and $\langle Q^2\rangle = 70.2$ GeV^2. Together with the data from Refs. [3,4] at lower values of Q, these distributions provide the first direct tests of the Q^2-dependence of $S_z^{NP}(b,Q,x)$. We therefore present a numerical value for the coefficient of $\ln Q/Q_0$ that yields reasonable agreement with all of the analyzed data. The resulting value of this coefficient differs significantly from the model parametrization in [1]. However, we should not draw too strong a conclusion from this difference, because it might be caused by ambiguities in the separation of Q^2 dependence and x dependence in the existing data. To draw a strong conclusion about the crossing symmetry model, experimental pseudorapidity distributions in a larger range of x at intermediate values of Q^2 will be needed.

From our analysis, we find that the data from Refs. [3,4] are consistent with the following parametrization of the nonperturbative Sudakov factor:

$$S_z^{NP}(b,Q,x) = b^2\left(0.013\frac{(1-x)^3}{x} + 0.19\ln\frac{Q}{Q_0} + C\right), \tag{35}$$

where the parameter Q_0 is fixed to be 2 GeV, and where we set $C=0$ for reasons explained later. In Figs. 1 and 2 we compare the resummed z-flow, calculated according to (28) and using the parametrization S_z^{NP} in (35), to the data from [4]. The z-flow is normalized by the inclusive DIS cross section $d\sigma/(dxdQ^2)$ (which will be denoted by the brief notation σ_{tot}).

Following the recent H1 publication [4], we organize these data into two sets of bins for fixed x and Q^2. One set covers $3.2 < \langle Q^2 \rangle < 70.2$ GeV^2 and $8\times10^{-5} < \langle x \rangle < 7\times10^{-3}$, out of which we consider the bins with $\langle Q^2 \rangle \geq 13.1$ GeV^2. The other set covers $175 < \langle Q^2 \rangle < 2200$ GeV^2 and $0.0043 < \langle x \rangle < 0.11$. The transformation of the experimental $d\langle E_T \rangle / d\eta^{cm}$ distributions into $d\Sigma_z/dq_T$ distributions and the calculation of the theoretical distributions $d\Sigma_z/dq_T$ are done using the mean values $\langle x \rangle$ and $\langle Q^2 \rangle$ for each bin published in [4]. In seven of the nine low-Q^2 bins (Fig. 1) we also show the earlier published data from [3].

Let us discuss the features of the data presented in Figs. 1 and 2. First, the data in the low-Q^2 bins is significantly influenced by nonperturbative effects and therefore is sensitive to the details of the parametrization of the nonperturbative Sudakov factor $S_z^{NP}(b, Q, x)$. This feature can be seen from the abundance of data points around the maximum of the q_T-distribution, where the shape is mainly determined by the nonperturbative Sudakov factor. Also, the low-Q^2 data from HERA is characterized by small values of x, between 10^{-4} and 10^{-2}. As we noticed in our earlier work [1], for the theory to be consistent with the data in this range of x, the nonperturbative Sudakov factor must increase rapidly as $x \to 0$, at least as $1/\sqrt{x}$ (*cf.* Eq. (22)). In our new analysis, we find that growth of $S_z^{NP}(b, Q, x)$ as $1/x$ at small x is in better agreement with the more recent data from [4].

Secondly, the data in the high-Q^2 bins of Fig. 2 shows a behavior that is qualitatively different from Fig. 1. In the region covered by the experimental data points, the q_T distribution is a monotonically decreasing function of q_T, which shows good agreement with the resummed z-flow over a significant range[3] of q_T. In the region $q_T < 10$ GeV, *i.e.*, where the maximum of the q_T distribution is located and where nonperturbative effects are important, the experimental q_T-bins are too large to provide any information about the shape of $d\Sigma_z/dq_T$. Thus, as mentioned earlier, the published high-Q^2 z-flow data from Ref. [4] is not sensitive to the dynamics described by the nonperturbative Sudakov factor $S_z^{NP}(b, Q, x)$.

A third comment is that most of the high-Q^2 data points in Fig. 2 correspond to $\langle x \rangle > 10^{-2}$. If the resolution of the H1 measurements at high Q^2 were better in the small-q_T region, then the high-Q^2 data would also reveal the behavior of $S_z^{NP}(b, Q, x)$ at large x. But, as mentioned before, the published data in the high-Q^2 bins are not very sensitive to the shape of the z-flow at small q_T. Therefore it is not possible to impose any constraints on $S_z^{NP}(b, Q, x)$ at large values of x, except that it should be positive, $S_z^{NP}(b, Q, x) > 0$. For this reason we have chosen a parametrization of the x-dependent part of $S_z^{NP}(b, Q, x)$ in (35) such that $S_z^{NP}(b, Q, x)$ grows approximately as $1/x$ as $x \to 0$ and is positive for all x. For the same reason, we chose $C = 0$ in the parametrization (35). Although the most general parametrization of $S_z^{NP}(b, Q, x)$ can have $C \neq 0$, the current data cannot distinguish between the parametrization (35) with $C = 0$ and $C \neq 0$, as long as the value of C is not very large.

---

[3] We point out once again that both the $\mathcal{O}(\alpha_s)$ and resummed z-flow lie below the data at very large q_T, in all bins of x and Q^2 in Figures 1 and 2.

How trustworthy is the resummed z-flow at large q_T?

As noted earlier, the $\mathcal{O}(\alpha_s)$ fixed-order z-flow is much larger than the data in the region $q_T/Q \ll 1$ and much smaller than the data in the region $q_T/Q \gtrsim 1$. In the small-q_T region, the resummed z-flow is, by its construction, more reliable than the fixed-order result. In the large-q_T region, the resummed z-flow, with the kinematical correction (33) included, is also in better agreement with the data than the fixed-order calculation. But theoretically, the resummed z-flow at large q_T/Q is not absolutely trustworthy, because it does not include those parts of the fixed-order z-flow that are subleading in the limit $q_T \to 0$, but which might be important at large q_T. If the NLO result were in a good agreement with the data at large q_T, it would be justified to consider it a more reliable prediction in this region. But since the $\mathcal{O}(\alpha_s)$ contribution is systematically smaller than the data, higher-order corrections are presumably necessary in order to describe the region $q_T \gtrsim Q$ reliably.

A systematic approach for improving the theoretical description of the large-q_T region would require inclusion of the complete $\mathcal{O}(\alpha_s^2)$ terms in both the fixed-order and resummed z-flows. But because such a calculation is not available, it might be beneficial to use the resummed z-flow as a better theoretical prediction both in the region $q_T/Q \ll 1$, where application of the resummation formalism is fully justified, and for q_T up to several units of Q, where the resummed z-flow agrees with the data better than the fixed-order one. Then the use of the resummed q_T-distributions of the z-flow will provide more reliable predictions for other observables relevant to the sDIS process.

As an example, resummation can improve the reliability of the theoretical prediction for the azimuthal asymmetry of the z-flow. The b-space resummation formalism affects only the coefficient ${}^1V_{zA}$ of the angular function $A_1(\psi,\varphi)$. This coefficient is the one that dominates the φ-integrated z-flow in the small-q_T region, where the energy flow is the most intense. On the other hand, the main goal of the measurement of angular asymmetries is to study structure functions other than ${}^1V_{zA}$, *e.g.,* those corresponding to the angular functions $A_3(\psi,\varphi) = -\cos\varphi \sinh 2\psi$ and $A_4(\psi,\varphi) = \cos 2\varphi \sinh^2\psi$. By using a better approximation for the coefficient ${}^1V_{zA}$, it is possible to measure the coefficients ${}^{3,4}V_{zA}$ more reliably. Conversely, by knowing that the all-order resummation effects are important in the region of small q_T and by concentrating on the region where q_T is of the order Q or larger, one may find angular asymmetries that are well approximated in the lowest orders of perturbative QCD. We discuss the impact of resummation on the angular asymmetries in more detail in another paper [14].

IV. DISTRIBUTIONS OF CHARGED PARTICLE MULTIPLICITY

Let us now turn to the discussion of semi-inclusive DIS cross sections. Although the resummation formalism, as outlined in Section II, can describe the cross section for any massless final-state particle (provided that the fragmentation functions for this particle are known), in this Section we will concentrate on distributions of the charged particle multiplicity, defined as

$$\frac{1}{\sigma_{tot}} \frac{d\sigma(A + l \to h^\pm + l' + X)}{d\Theta}. \tag{36}$$

Here Θ is some kinematical variable, such as the variable q_T^2 in Eq. (2), the transverse momentum p_T of the final-state charged particle in the hCM frame, or the Feynman variable x_F, defined by

$$x_F \equiv \frac{2p_B^z}{W} = z\left(1 - \frac{q_T^2}{W^2}\right). \tag{37}$$

In (37) p_B^z is the longitudinal component of the momentum of the final-state hadron in the hCM frame. For small values of q_T, *i.e.,* in the region with the highest rate,

$$x_F \approx z. \tag{38}$$

In our calculation we assume that the charged particles registered in the detector are mostly charged pions, kaons and protons. Therefore the cross section for charged particle production can be calculated using (5) with the replacement of the fragmentation functions $D_{B/b}(\xi_b, \mu_F)$ by

$$D_{h^\pm/b}(\xi_b, \mu_F) = \sum_B D_{B/b}(\xi_b, \mu_F). \tag{39}$$

The fragmentation functions $D_{B/b}(\xi_b, \mu_F)$ are known reasonably well only for $\xi_b \gtrsim 0.05 - 0.1$ [19–21]. Thus, the formalism presented here is applicable to the production of charged particles with sufficiently large energies, *i.e.*, for $z \gtrsim 0.05$.

Certain experimental distributions are readily available from the literature [5,17,18], such as $d\sigma/dp_T$, $d\sigma/dx_F$, as well as distributions for the average transverse momentum $\langle p_T^2 \rangle$. However, the "experimental" q_T distributions must currently be derived from pseudorapidity distributions by using Eq. (4). Although the distributions $d\sigma/dp_T$ and $\langle p_T^2 \rangle$ are quite sensitive to resummation effects, they cannot be interpreted as easily as the distributions $d\sigma/dq_T$, primarily because the distributions $d\sigma/dp_T$ and $\langle p_T^2 \rangle$ mix resummation effects at small values of q_T with perturbative contributions from the region $q_T/Q \gtrsim 1$. The most straightforward way to study the effects of multiple parton radiation would be to consider the q_T (or pseudorapidity) distributions that satisfy the additional requirement $z > 0.05 - 0.1$ and that are organized into small bins of Q^2 and x. Unfortunately, such distributions have not been published yet.

Because the experimental q_T distributions are unavailable, we have decided to undertake a simpler analysis than the one presented for the energy flow. Our goal here is to understand how the multiple parton radiation *could* affect various aspects of charged particle production. For this purpose we focus our attention on data from the ZEUS Collaboration [5], which presents the charged particle multiplicity in a phase-space region characterized by the mean values $\langle W \rangle = 120$ GeV, $\langle Q^2 \rangle = 28$ GeV^2, and the additional constraint $z > 0.05$. These values of $\langle W \rangle$ and $\langle Q^2 \rangle$ translate into an average value of $x = 1.94 \times 10^{-3}$. Within the framework of a simple model for nonperturbative effects at small q_T, we will demonstrate that resummation describes qualitative features of this set of experimental data better than the fixed-order calculation. In all of the cases presented, our strategy is to compare the resummed multiplicity to that from the next-to-leading order calculation. In the numerical analysis, the multiplicity was calculated using the CTEQ5M1 PDFs [16] and the FFs from [20]. For the resummed multiplicity, the "canonical" combination $C_1/C_2 = \mu_F b = 2e^{-\gamma_E}$

was used. Unless specified, the NLO cross section was calculated according to (18), with the parameter $q_T^{sep} = 1.2$ GeV, and for the factorization scale $\mu_F = Q$.

As in the case of the z-flow, the resummed charged particle multiplicity may suffer from matching ambiguities at $q_T/Q \sim 1$. In Section III, we found that the resummed z-flow is in better agreement with the experimental $d\sigma/dq_T$ distributions than the NLO z-flow, for the whole range $q_T/Q \lesssim 2-4$. That result suggests that it might be preferable to use the resummed z-flow in the whole range $q_T/Q \lesssim 2-4$ as a better theoretical prediction, until the $\mathcal{O}(\alpha_s^2)$ prediction for the z-flow in the region $q_T/Q \gtrsim 1$ becomes available. In the case of the charged particle multiplicity, the resummed cross section, which is calculated according to the formula

$$\frac{d\sigma_{BA}}{dxdzdQ^2dq_T^2d\varphi} = \frac{\sigma_0 F_l}{S_{eA}} \frac{A_1(\psi,\varphi)}{2} \int \frac{d^2b}{(2\pi)^2} e^{i\vec{q}_T\cdot\vec{b}} \widetilde{W}_{BA}(b,x,z,Q) + Y_{BA}, \tag{40}$$

overestimates the experimentally measured rate for the production of charged particles with $p_T > 2$ GeV. This discrepancy indicates that the resummed cross section in the region $q_T/Q \gtrsim 1$ is too high, so that switching to the perturbative cross section in this region is in fact required. Therefore, we have chosen to use the resummed cross section for $q_T \leq 5$ GeV and switch to the next-to-leading order cross section for $q_T \geq 5$ GeV.

As in the case of the z-flow, the shape of the q_T distribution for the charged particle multiplicity at small values of q_T depends strongly on the unknown nonperturbative Sudakov factor $S^{NP}(b,Q,x,z)$. For the purposes of this study, we introduce a preliminary parametrization of the nonperturbative Sudakov factor for the *fixed* values of $x = 1.94\times10^{-3}$ and $Q^2 = 28$ GeV^2, *i.e.,* the values that coincide with the average values of x and Q^2 in [5]. This *z-dependent* parametrization is

$$S^{NP}\left(b, Q^2 = 28 \text{ GeV}^2, x = 1.94\times10^{-3}, z\right) = b^2\left(0.18 + 0.8\frac{(1-z)^3}{z^{1.4}}\right). \tag{41}$$

Since the ZEUS Collaboration did not publish pseudorapidity distributions for the charged particle multiplicity $(1/\sigma_{tot})d\sigma/d\eta^{cm}$ in bins of varying z, we had to deduce information about the z-dependence of S^{NP} from the less direct distribution of $\langle p_T^2\rangle$ vs. x_F presented in Fig. 3c of [5]. This distribution, known as a "seagull" for its characteristic shape (Fig. 3a), can be converted into the more illustrative distribution of $\langle q_T^2\rangle$ vs. x_F (Fig. 3b). Since the major portion of the registered events comes from the region $q_T^2/W^2 \ll 1$, or $x_F \approx z$, a first estimate of the experimental data points for the distribution of $\langle q_T^2\rangle$ vs. x_F can be obtained by assuming that

$$\langle q_T^2\rangle \approx \frac{\langle p_T^2\rangle}{\langle z\rangle^2} \approx \frac{\langle p_T^2\rangle}{\langle x_F\rangle^2}, \tag{42}$$

where $\langle x_F\rangle$ denotes central values of x_F in each bin in Fig. 3a.[4] We refer to the resulting values as "derived data".

[4] In principle, a more accurate experimental distribution $\langle q_T^2\rangle$ vs. x_F can be determined by its direct measurement.

Note that the shapes of $\langle p_T^2 \rangle$ vs. x_F and $\langle q_T^2 \rangle$ vs. x_F are quite different. The transformation from Fig. 3a to Fig. 3b shows immediately that the wing-like shape of the distribution of $\langle p_T^2 \rangle$ vs. x_F should be attributed to a purely kinematical effect, namely an extra factor $1/z^2$ which is absent in the distribution of $\langle q_T^2 \rangle$ vs. x_F. Once this extra factor is removed, we see from Fig. 3b that $\langle q_T^2 \rangle$ increases monotonically and rapidly as z approaches zero. In other words, the q_T distribution broadens rapidly when z decreases. This behavior is approximately realized by the simple z-dependent nonperturbative Sudakov factor $S^{NP}(b, Q, x, z)$ given in Eq. (41).

The shape of the resummed cross section at $q_T \leq 5$ GeV and the parametrization of $S^{NP}(b, Q, x, z)$ were chosen to maximize the agreement between the resummed distribution of $\langle q_T^2 \rangle$ vs. x_F and the "derived data" (*cf.* Fig. 3b). Figure 3b shows that the resummed calculation is in better agreement with the data points than the NLO expression. We have found it difficult to reproduce the rapid growth of $\langle q_T^2 \rangle$ as $x_F \to 0$ in either approach. In the future, it will be interesting to see how a more precise theoretical study will be able to adequately explain this rapid growth of $\langle q_T^2 \rangle$ in the region $x_F \to 0$, assuming that the actual experimental data for the $\langle q_T^2 \rangle$ vs. x_F distribution resemble the "derived data" discussed above.

The resummation also significantly affects the p_T dependence of the charged particle multiplicity. In Fig. 4 we present the distribution $(1/\sigma_{tot}) d\sigma/dp_T$. We see that resummation effects must be included to describe the shape of this distribution at $p_T \leq 1$ GeV. Furthermore, resummation also improves the agreement between the theory and the experiment in the whole range of p_T. Through Eq. (55), the improved description of the q_T distribution in the small-q_T region translates into a better agreement with the p_T distribution in the whole range of p_T. Just as in the case of the z-flow, the fixed-order calculation gives a rate that is too small compared to the data, which implies that higher-order corrections are important. Until the complete $\mathcal{O}(\alpha_s^2)$ corrections are available, the resummation formalism, which already accounts for the most important contributions in the region of the phase space with the highest rate (*i.e.,* at small q_T), serves as a better theoretical prediction in the whole range of p_T.

Finally, Fig. 5 shows the x_F-distribution for the charged particle multiplicity $(1/\sigma_{tot}) d\sigma/dx_F$. We see that both the resummed and fixed-order distributions are in reasonable agreement with the data and with earlier published theoretical results for the $\mathcal{O}(\alpha_s)$ x_F-distributions [15]. For the fixed-order multiplicity, we present two additional curves corresponding to different choices of the factorization scale μ_F in (5); the lower and upper dotted curves correspond to $\mu_F = 0.5Q$ and $2Q$, respectively. Note that the scale dependence of the NLO multiplicity increases when $z \to 0$. Also note that the resummed multiplicity is significantly lower than the data in the two lowest bins of x_F ($\langle x_F \rangle = 0.075$ and 0.125), but consistent with the NLO multiplicity within the uncertainty due to the scale dependence. Such behavior of the resummed multiplicity results from the dependence of the $\mathcal{O}(\alpha_s)$ coefficient functions $\mathcal{C}_{ba}^{out(1)}(\hat{z}, C_1, C_2, b_*, \mu_F)$ on the additional term $\ln \hat{z}$ which was given in Eqs. (72) and (73) and discussed at the end of Section II. This negative logarithm dominates the $\mathcal{C}^{out(1)}$-functions at very small values of $\hat{z}$. Similarly, the integral (12) of the NLO cross

section over the lowest bin $0 \le q_T^2 \le (q_T^{sep})^2$ depends on $\ln \widehat{z}$ through the terms

$$-\frac{\alpha_s}{2\pi} \ln \frac{\mu_F^2}{(\widehat{z}\, q_T^{sep})^2} \Big(\delta(1-\widehat{z}) \delta_{bj} P_{ja}(\widehat{x}) + P_{bj}(\widehat{z}) \delta(1-\widehat{x}) \delta_{ja} \Big),$$

as given in (14). Numerically, this dependence is less pronounced than in the resummed cross section. For $z \lesssim 0.1$, the growing scale dependence of the multiplicity in the $\mathcal{O}(\alpha_s)$ calculation indicates that unaccounted higher-order effects become important and are needed to improve the theory predictions. For example, including the $\mathcal{O}(\alpha_s^2)$ coefficient $\mathcal{C}_{ba}^{(2)}$ in the resummed calculation will be necessary to improve the description of the charged particle multiplicity in the small-z region.

V. DISCUSSION AND CONCLUSIONS

In this paper we have continued the discussion of the effects of multiple parton radiation in semi-inclusive deep-inelastic scattering that was started in [1]. We have demonstrated that these effects influence a large class of observables and can be described with the help of a resummation formalism [8] that is similar to the resummation formalism used to improve the theoretical description of energy-energy correlations in e^+e^- hadroproduction [11], and small-p_T vector boson production at hadron-hadron colliders [12].

Although this formalism needs further improvement, in particular in the procedure for matching the resummed curve with the perturbative result in the transition region, it already improves the agreement between the theory and the data and provides interesting insights about qualitative features of semi-inclusive DIS. We have demonstrated that the resummation formalism describes the pseudorapidity distributions of the transverse energy flow more accurately than the NLO calculation; this formalism also has good potential to improve the description of various distributions of particle multiplicity.

From our analysis we conclude that the experimentally measured q_T distribution for the energy flow broadens rapidly as $x \to 0$. This rapid broadening of the q_T distribution can be realized if the nonperturbative Sudakov factor in the resummed energy flow increases as $1/x$. Similarly, the q_T distribution for the charged particle multiplicity broadens rapidly when $z \to 0$, which is consistent with the nonperturbative Sudakov factor increasing as $z^{-1.4}$. The sDIS nonperturbative Sudakov factors at small values of x and z are therefore qualitatively different from the known nonperturbative Sudakov factors for vector boson production and e^+e^- hadroproduction, which do not depend on the longitudinal variables at all. The rapid growth of the nonperturbative Sudakov factor in sDIS might indicate that the ep collider HERA tests the resummation formalism in a new dynamical regime, which was not studied yet at colliders of other types.

There are several theoretical aspects of the resummation formalism that can be clarified when more experimental data are published. Perhaps the largest uncertainty in the predictions of the resummation formalism comes from the unknown nonperturbative contributions, which in the b-space formalism are included in the nonperturbative Sudakov factor $S^{NP}(b)$. In this paper, we have presented simple parametrizations of $S^{NP}(b)$ for the transverse energy flow (cf. Eq. (35)) and charged particle multiplicity (cf. Eq. (41)). These parametrizations

were found by fitting the resummed energy flow and charged particle multiplicity to the data from Refs. [3,4] and Ref. [5], respectively. Experimental measurements outside the range of those data will make it possible to further improve these parametrizations and, hence, the accuracy of the resummation formalism.

The most straightforward way to study $S^{NP}(b)$ is by measuring the variation of the q_T spectra of physical quantities due to variations of one kinematical variable, with other variables fixed or varying only in a small range. For the energy flow, it would be beneficial to obtain more data at $x > 10^{-2}$, where the predictions of the resummation formalism can be tested more reliably, without potential uncertainties due to the small-x physics. Another interesting question is the dependence of the nonperturbative Sudakov factor on the virtuality Q of the vector boson. This dependence can be tested by studying the q_T spectra in a range of Q with sufficient experimental resolution in the current fragmentation region. Finally, to study effects of multiple parton radiation on semi-inclusive production of individual hadrons, it will be interesting to see the q_T spectra for particle production multiplicities with the additional constraint $z > 0.05 \sim 0.1$, *i.e.,* in the kinematical region where the parametrizations of the fragmentation functions are known reasonably well.

ACKNOWLEDGEMENTS

We would like to thank J. Collins, D. Soper, G. Sterman and other members of the CTEQ Collaboration for useful discussions. The authors also thank S. Kretzer for providing a Fortran code with the parametrizations of the fragmentation functions. This work was supported under the NSF grant PHY-9802564.

APPENDIX A: SUMMARY OF NOTATIONS

Detailed explanations of the notations are provided in [1].

We limit the discussion to the case of the semi-inclusive DIS process

$$e + A \to e + B + X \tag{43}$$

at the ep collider HERA. Here e is an electron or positron, A is a proton, B is a hadron observed in the final state, and X represents any other particles in the final state in the sense of inclusive scattering. We denote the momenta of A and B by p_A^μ and p_B^μ, and the momenta of the lepton in the initial and final states by l^μ and l'^μ. Also, q^μ is the momentum transfer to the hadron system, $q^\mu = l^\mu - l'^\mu$. We assume that the initial lepton and hadron interact only through a single photon exchange. Therefore, q^μ also has the meaning of the 4-momentum of the exchanged virtual photon γ^*.

The kinematics of the process (43) can be discussed conveniently with the help of the following five Lorentz scalars:

- the square of the center-of-mass energy $\sqrt{S_{eA}}$ of the initial hadron and lepton,

$$S_{eA} = (p_A + l)^2 = 2p_A \cdot l; \tag{44}$$

- the momentum transfer from the leptonic to the hadronic part of the process,

$$Q^2 = -q^2 = 2\ell \cdot \ell'; \tag{45}$$

- the Bjorken variable,

$$x = \frac{Q^2}{2p_A \cdot q}; \tag{46}$$

- a variable z describing energy transfer from the composite photon-proton intermediate state to the observed final hadron B,

$$z = \frac{p_B \cdot p_A}{q \cdot p_A} = \frac{2x p_B \cdot p_A}{Q^2}; \tag{47}$$

- a scale q_T that serves as a control parameter in the resummation formalism,

$$q_T^2 = -q_t^\mu q_{t\mu}, \tag{48}$$

where

$$q_t^\mu = q^\mu - p_A^\mu \frac{q \cdot p_B}{p_A \cdot p_B} - p_B^\mu \frac{q \cdot p_A}{p_A \cdot p_B}. \tag{49}$$

Let a denote the parton in A that participates in the hard scattering, with momentum $p_a^\mu = \xi_a p_A^\mu$. Let b denote the parton of which B is a fragment, with momentum $p_b^\mu = p_B^\mu/\xi_b$. We use the symbol "$\widehat{\ }$" to denote quantities at the parton level. Correspondingly, we introduce the parton-level Lorentz scalars $\widehat{x}$, $\widehat{z}$ that are analogous to the hadron-level scalars $x,\ z$:

$$\widehat{x} = \frac{Q^2}{2p_a \cdot q} = \frac{x}{\xi_a}, \tag{50}$$

$$\widehat{z} = \frac{p_b \cdot p_a}{q \cdot p_a} = \frac{z}{\xi_b}. \tag{51}$$

The paper concentrates on the discussion of experimental data presented in the hadronic center-of-mass (hCM) coordinate system, which is defined to be the center-of-mass frame of the proton A and the virtual photon γ^*, with the z axis pointing in the direction of the photon's momentum. The momenta of A and γ^* in the hCM frame are

$$p_A^\mu = \left\{\frac{W^2+Q^2}{2W}, 0, 0, -\frac{W^2+Q^2}{2W}\right\}, \tag{52}$$

$$q^\mu = \left\{\frac{W^2-Q^2}{2W}, 0, 0, \frac{W^2+Q^2}{2W}\right\}, \tag{53}$$

where

$$W \equiv Q\sqrt{\frac{1}{x}-1}. \tag{54}$$

The momentum of the outgoing hadron B in this frame lies in the xz plane, and its component perpendicular to the z axis is

$$p_T = zq_T. \tag{55}$$

The energy and longitudinal component of the momentum of B are

$$E_B = z\frac{W^2+q_T^2}{2W}, \tag{56}$$

$$p_B^z = z\frac{W^2-q_T^2}{2W}. \tag{57}$$

The pseudorapidity of B in this frame is simply related to q_T, by

$$q_T = We^{-\eta_{cm}}. \tag{58}$$

The region of small q_T, where our resummation calculation is relevant, corresponds to the region of large pseudorapidity in the hCM frame.

We denote by φ the angle between the xz plane (the plane of the momenta $\vec{p}_A$ and $\vec{p}_B$) and the plane of the lepton momenta $\vec{\ell}$ and $\vec{\ell}'$. In terms of the angle φ and the boost parameter $\psi = \cosh^{-1}(2xS_{eA}/Q^2 - 1)$, the momenta of the leptons in the hCM frame are

$$\begin{aligned} l^\mu &= \left\{\frac{1}{4W}\Big((W^2+Q^2)\cosh\psi + W^2 - Q^2\Big), \frac{Q}{2}\sinh\psi\cos\varphi, -\frac{Q}{2}\sinh\psi\sin\varphi,\right. \\ &\quad \left.\frac{1}{4W}\Big((W^2+Q^2) + (W^2-Q^2)\cosh\psi\Big)\right\}; \end{aligned} \tag{59}$$

$$\begin{aligned} l'^\mu &= \left\{\frac{1}{4W}\Big((W^2+Q^2)\cosh\psi - W^2 + Q^2\Big), \frac{Q}{2}\sinh\psi\cos\varphi, -\frac{Q}{2}\sinh\psi\sin\varphi,\right. \\ &\quad \left.\frac{1}{4W}\Big(-W^2 - Q^2 + (W^2-Q^2)\cosh\psi\Big)\right\}. \end{aligned} \tag{60}$$

It is convenient to decompose the sDIS cross section into a sum over a complete set of functions $A_\rho(\psi,\varphi)$ of the azimuthal angle φ and the parameter ψ [7]:

$$\frac{d\sigma_{BA}}{dxdzdQ^2dq_T^2d\varphi} = \sum_\rho {}^\rho V_{BA}(x,z,Q^2,q_T^2)A_\rho(\psi,\varphi). \tag{61}$$

If the scattering of leptons on hadrons is caused by a parity-conserving interaction, then the spin-averaged sDIS cross section receives contributions only from four angular functions $A_\rho(\psi,\varphi)$, which are

$$\begin{aligned} A_1 &= 1+\cosh^2\psi, \\ A_2 &= -2, \\ A_3 &= -\cos\varphi\sinh 2\psi, \\ A_4 &= \cos 2\varphi\sinh^2\psi. \end{aligned} \tag{62}$$

Since the angular functions A_3 and A_4 are proportional to $\cos\varphi$ and $\cos 2\varphi$, respectively, they do not contribute to the cross section that is integrated over the azimuthal angle φ. Hence, the φ-integrated cross section $d\sigma/(dxdzdQ^2dq_T^2)$ depends only on the structure functions A_1 and A_2.

APPENDIX B. PERTURBATIVE COEFFICIENTS IN THE RESUMMED CROSS SECTION

The Wilson coefficient functions $\mathcal{C}_{ba}^{in}$ and $\mathcal{C}_{ba}^{out}$, and the perturbative part $S^P(b,Q)$ of the Sudakov factor in (20) can be expanded in powers of α_s [8,1], as

$$\begin{aligned} S^P(b,Q,C_1,C_2) &= \int_{C_1^2/b^2}^{C_2^2Q^2} \frac{d\overline{\mu}^2}{\overline{\mu}^2} \sum_{k=1}^{\infty} \left(\frac{\alpha_s(\mu)}{\pi}\right)^k \Big\{ A^{(k)}(\alpha_s(\overline{\mu}),C_1) \ln\frac{C_2^2Q^2}{\overline{\mu}^2} \\ &+ B^{(k)}(\alpha_s(\overline{\mu}),C_1,C_2)\Big\}; \end{aligned} \tag{63}$$

$$\mathcal{C}_{ba}^{in}(\widehat{x},C_1,C_2,b,\mu_F) = \sum_{k=0}^{\infty} \mathcal{C}_{ba}^{in(k)}(\widehat{x},\mu_F b)\left(\frac{\alpha_s(\mu_F)}{\pi}\right)^k; \tag{64}$$

$$\mathcal{C}_{ba}^{out}(\widehat{z},C_1,C_2,b,\mu_F) = \sum_{k=0}^{\infty} \mathcal{C}_{ba}^{out(k)}(\widehat{z},\mu_F b)\left(\frac{\alpha_s(\mu_F)}{\pi}\right)^k. \tag{65}$$

Up to the order $\mathcal{O}(\alpha_s)$, the coefficients in Eqs. (63)-(65) are listed below.

- For the Sudakov factor,

$$A^{(1)} = C_F, \tag{66}$$

$$B^{(1)} = 2C_F \ln\Big(\frac{e^{-3/4}C_1}{b_0 C_2}\Big). \tag{67}$$

  Here $C_F = 4/3$ is a color factor; μ_F is a factorization scale; $b_0 = 2e^{-\gamma_E}$; C_1 and C_2 are constants that are conventionally chosen such that $C_1/C_2 = b_0$.

- For the coefficient functions,

$$\mathcal{C}_{ij}^{in(0)}(\xi,\mu_F b) = \mathcal{C}_{ij}^{out(0)}(\xi,\mu_F b) = \delta_{ij}\delta(1-\xi), \tag{68}$$

$$\mathcal{C}_{ag}^{in(0)} = \mathcal{C}_{ga}^{out(0)} = 0, \tag{69}$$

$$\begin{aligned} \mathcal{C}_{ij}^{in(1)}(\widehat{x},\mu_F b) &= \frac{C_F}{2}(1-\widehat{x}) - P_{qq}(\widehat{x})\ln\Big(\frac{\mu_F b}{b_0}\Big) \\ &- C_F\delta(1-\widehat{x})\Big(\frac{23}{16} + \ln^2\Big(\frac{e^{-3/4}C_1}{b_0 C_2}\Big)\Big), \end{aligned} \tag{70}$$

$$\mathcal{C}_{jg}^{in(1)}(\widehat{x},\mu_F b) = \frac{1}{2}\widehat{x}(1-\widehat{x}) - P_{qg}(\widehat{x})\ln\Big(\frac{\mu_F b}{b_0}\Big), \tag{71}$$

$$\mathcal{C}_{ij}^{out(1)}(\widehat{z},\mu_F b) = \frac{C_F}{2}(1-\widehat{z}) - P_{qq}(\widehat{z})\ln\Big(\frac{\mu_F b}{b_0\widehat{z}}\Big)$$

$$- \; C_F\delta(1-\widehat{z})\Big(\frac{23}{16}+\ln^2\Big(\frac{e^{-3/4}C_1}{b_0C_2}\Big)\Big), \tag{72}$$

$$\mathcal{C}_{gj}^{out(1)}(\widehat{z},\mu_F b) \;=\; \frac{C_F}{2}\widehat{z} - P_{gq}(\widehat{z})\ln\Big(\frac{\mu_F b}{b_0\widehat{z}}\Big), \tag{73}$$

$$\mathcal{C}_{gg}^{in(1)} \;=\; \mathcal{C}_{gg}^{out(1)} = 0. \tag{74}$$

Here P_{qq} and P_{qg} are one-loop splitting functions [9]. The subscripts a, b correspond to quarks, antiquarks and gluons; the subscripts i, j correspond to the quarks and antiquarks only.

REFERENCES

[1] P.M. Nadolsky, D.R. Stump, C.P. Yuan, Phys.Rev. D61, 014003 (2000).

[2] H1 Coll., Z. Phys. C63, 377 (1994); C70, 609 (1996); C72, 573 (1996); Phys. Lett. B328, 176 (1994); Nucl. Phys. B485, 3 (1997).

[3] H1 Coll., Phys. Lett. B356, 118 (1995).

[4] H1 Coll., Eur. Phys. J., C12, 595 (2000).

[5] ZEUS Coll., Z. Phys. C70, 1 (1996).

[6] ZEUS Coll., Phys.Lett. B481, 199 (2000).

[7] R. Meng, F. Olness, D. Soper, Nucl. Phys. B371, 79 (1992).

[8] R. Meng, F. Olness, D. Soper, Phys.Rev. D54, 1919 (1996); see also J. Collins, Nucl. Phys. B396, 161 (1993).

[9] Yu.L. Dokshitzer, JETP 46, 641 (1977); V.N. Gribov, L.N. Lipatov, Sov. Journ. Nucl. Phys. 15, 78 (1972); G. Altarelli, G. Parisi, Nucl. Phys. B126, 298 (1977).

[10] C. Balazs, C.-P. Yuan, Phys. Rev. D56, 5558 (1997).

[11] J. Collins, D. Soper, Nucl. Phys. B193, 381 (1981); B197, 446 (1982).

[12] J. Collins, D. Soper, G. Sterman, Nucl. Phys. B250, 199 (1985).

[13] The energy flow normalized according to Eq. (23) was originally used in R.D. Peccei, R. Rückl, Phys. Lett. B84 (1979) 95; Phys. Rev. D20, 1235 (1979); Nucl. Phys. B162, 125 (1980); M. Dechantsreiter, F. Halsen, D.M. Scott, Z. Phys. C8, 85 (1981).

[14] P.M. Nadolsky, D.R. Stump, C.P. Yuan, hep-ph/0012262.

[15] D. Graudenz, Phys. Lett. B406, 178 (1997); Fortsch.Phys. 45, 629 (1997).

[16] H.L. Lai et al., CTEQ Coll., Eur.Phys. J. C12, 375 (2000).

[17] EMC Coll., Z. Phys. C52, 361 (1991).

[18] E665 Coll., Z. Phys. C76, 441 (1997).

[19] J. Binnewies, B. A. Kniehl, G. Kramer, Phys. Rev. D52, 4947 (1995); B.A. Kniehl, G. Kramer, B. Potter, Nucl.Phys. B582, 514 (2000).

[20] S. Kretzer, Phys. Rev. D62, 054001 (2000).

[21] L. Bourhis et al., hep-ph/0009101.

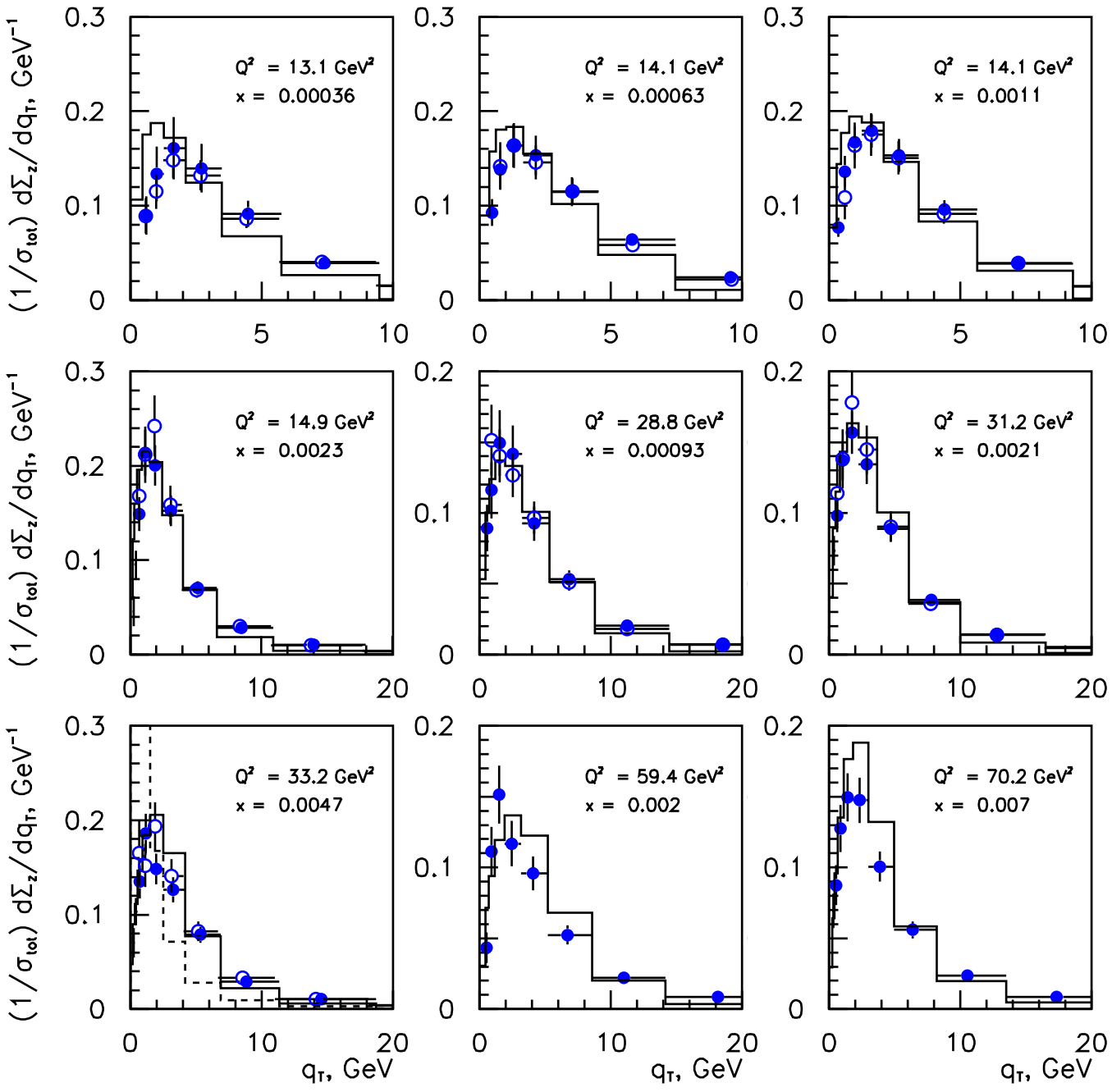

FIG. 1. Comparison of the resummed z-flow in the current region of the hCM frame with the data in the low-Q^2 bins from Refs. [4] (filled circles) and [3] (empty circles). The parametrization of the nonperturbative Sudakov factor in (35) is used. For the bin with $\langle Q^2\rangle = 33.2$ GeV^2 and $\langle x\rangle = 0.0047$, the $\mathcal{O}(\alpha_s)$ contribution for $\mu_F = Q$ is shown as a dashed curve.

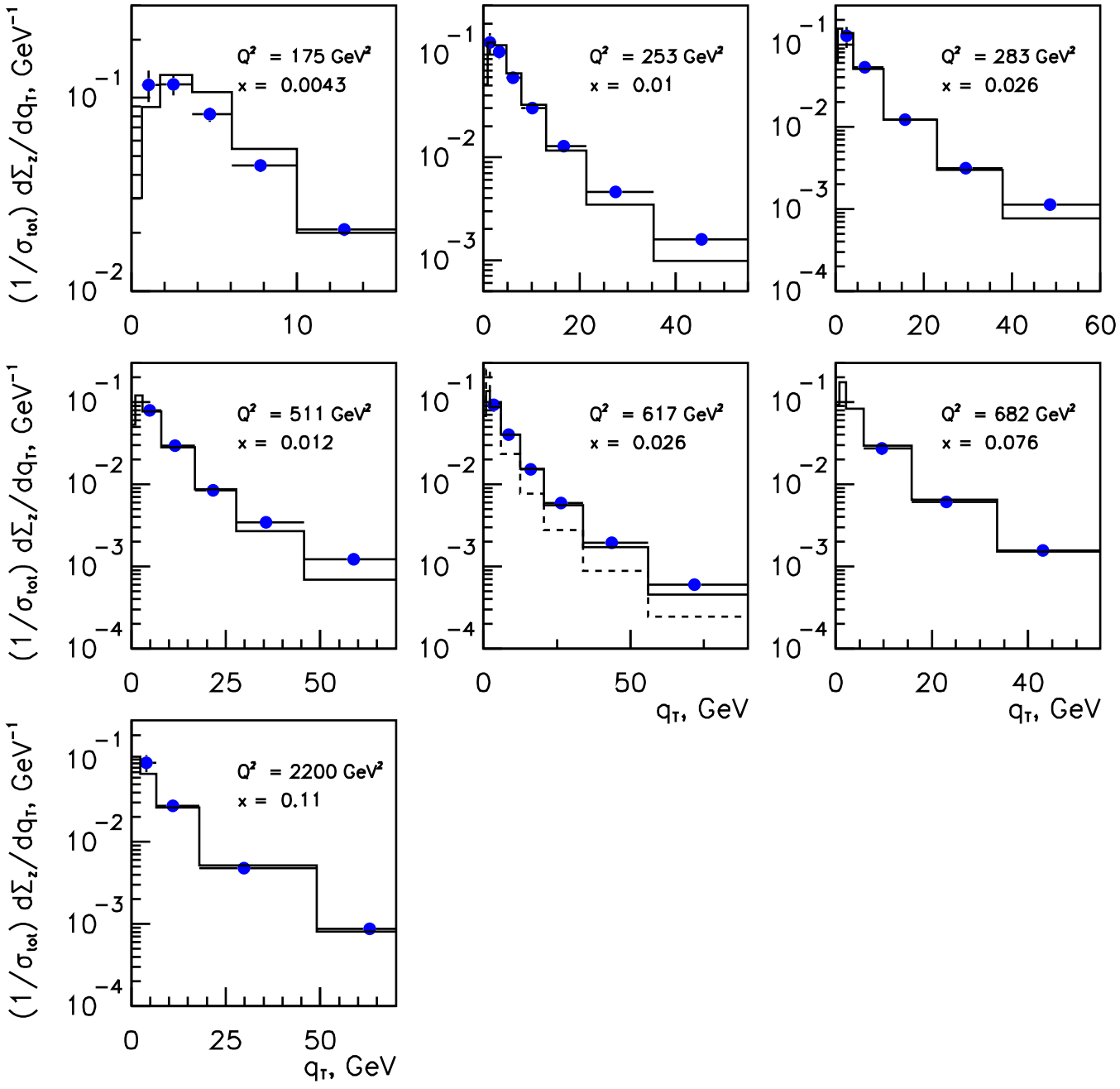

FIG. 2. Comparison of the resummed z-flow in the current region of the hCM frame with the data in the high-Q^2 bins from Ref. [4]. The parametrization of the nonperturbative Sudakov factor in (35) is used. For the bin with $\langle Q^2\rangle = 617$ GeV^2 and $\langle x\rangle = 0.026$, the $\mathcal{O}(\alpha_s)$ contribution for $\mu_F = Q$ is shown as a dashed curve.

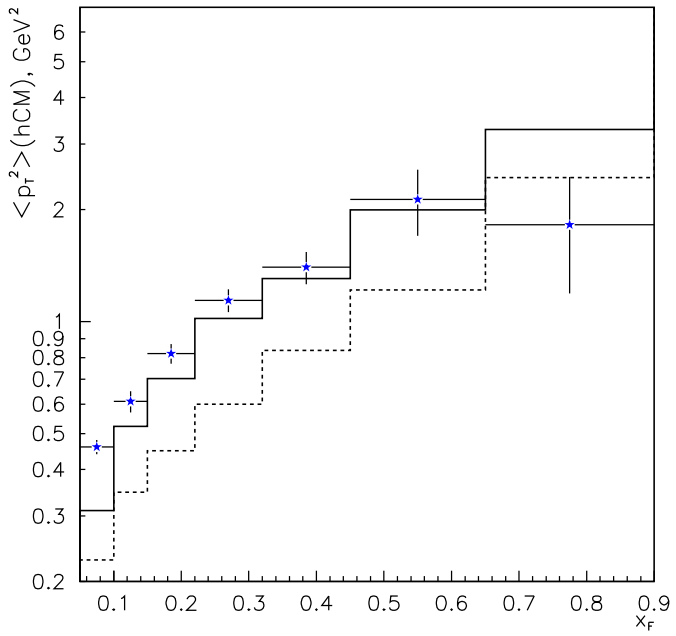

(a)

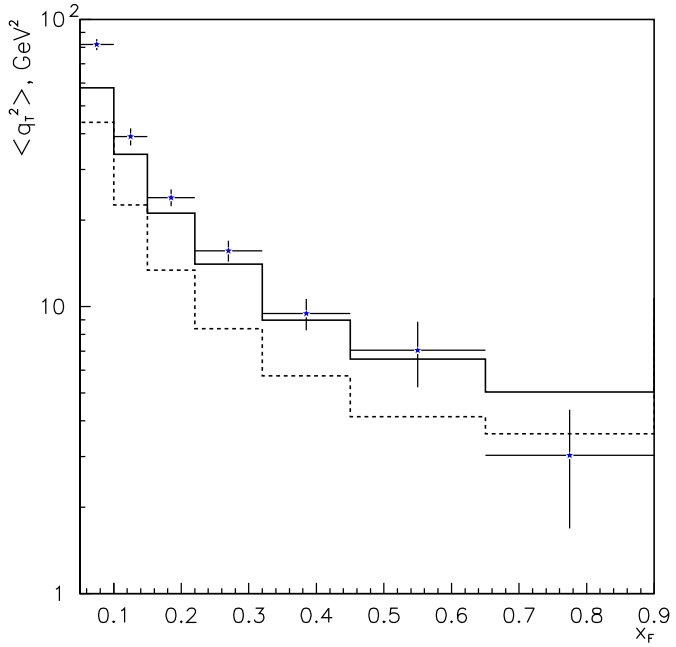

(b)

FIG. 3. The distributions (a) $\langle p_T^2 \rangle$ vs. x_F and (b) $\langle q_T^2 \rangle$ vs. x_F for the charged particle multiplicity at $\langle W \rangle = 120$ GeV, $\langle Q^2 \rangle = 28$ GeV^2. The experimental points for the distribution $\langle p_T^2 \rangle$ vs. x_F are from Fig. 3c of Ref. [5]. The "experimental" points for the distribution $\langle q_T^2 \rangle$ vs. x_F are derived using Eq. (42). The solid and dashed curves correspond to the resummed and the next-to-leading order ($\mu_F = Q$) multiplicity, respectively.

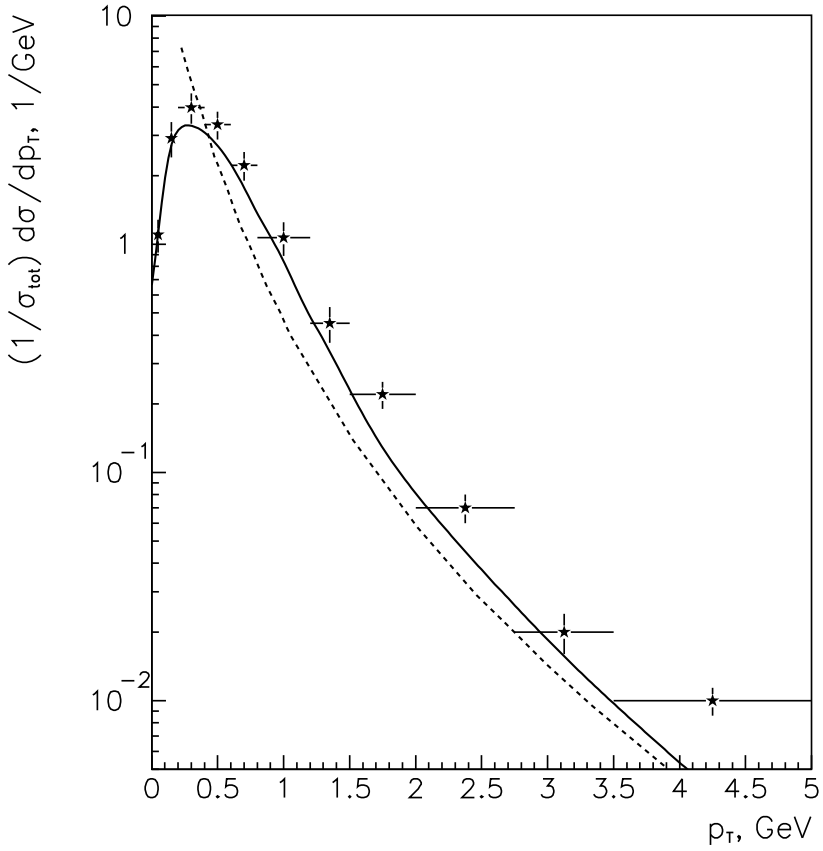

FIG. 4. The dependence of the charged particle multiplicity on the transverse momentum p_T of the observed particles in the hCM frame. The data points are from [5]. The solid and dashed curves correspond to the resummed and NLO multiplicities, respectively.

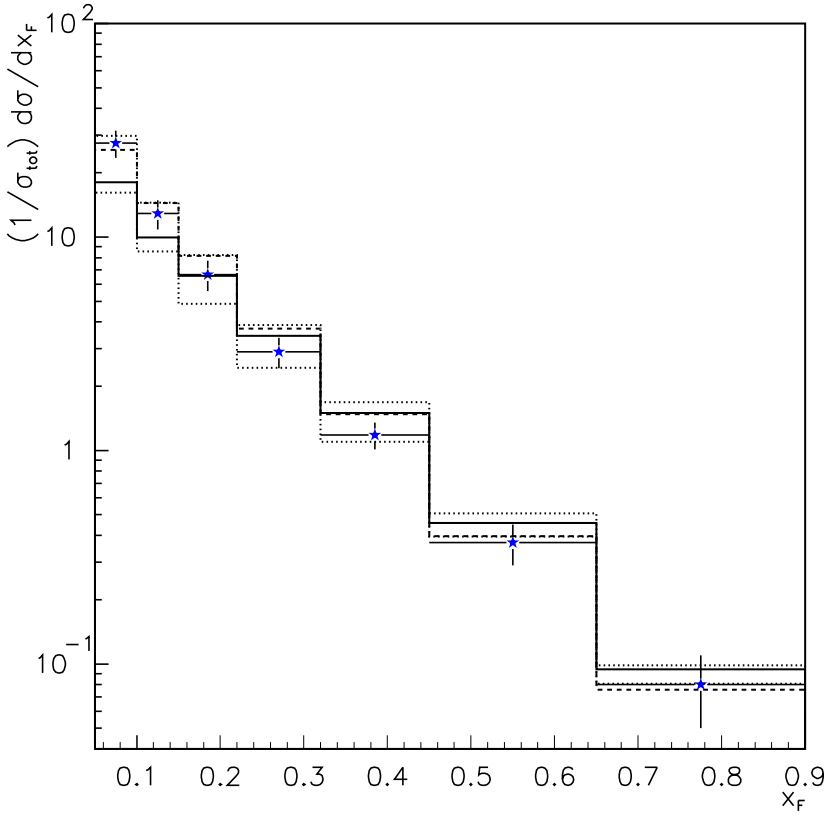

FIG. 5. The dependence of the charged particle multiplicity on the Feynman variable x_F in the hCM frame. The solid curve corresponds to the resummed multiplicity. The dashed, lower dotted and upper dotted curves correspond to the NLO multiplicity calculated for $\mu_F = Q,\ 0.5Q$ and $2Q$, respectively.